Dystrophin Is a Tumor Suppressor in Human Myogenic Cancers

Yuexiang Wang[1], Adrian Marino-Enriquez[1], Richard R. Bennett[2], Meijun Zhu[1], Yiping Shen[3], Grant Eilers[1], Benjamin Fletcher[1], Cristina R. Antonescu[4], Tamas Ordog[5], Christopher D.M. Fletcher[1], George D. Demetri[6], Louis M. Kunkel[2], Jonathan A. Fletcher[1*]

[1]Department of Pathology, Brigham and Women's Hospital and Harvard Medical School, Boston, MA, USA. [2]Program in Genomics and Division of Genetics, Howard Hughes Medical Institute and the Manton Center for Orphan Disease Research, Children's Hospital, Boston, MA, USA. [3]Genetic Diagnostic Laboratory, Department of Laboratory Medicine, Children's Hospital, Boston, MA, USA. [4]Departments of Pathology, Memorial Sloan - Kettering Cancer Center, New York, NY, USA. [5]Enteric Neuroscience Program and Department of Physiology and Biomedical Engineering, Mayo Clinic, Rochester, MN, USA. [6]Ludwig Center at Dana-Farber Cancer Center and Department of Medical Oncology, Dana-Farber Cancer Institute, Boston, MA, USA

ABSTRACT

Many common human mesenchymal tumors, including gastrointestinal stromal tumor (GIST), rhabdomyosarcoma (RMS), and leiomyosarcoma (LMS), feature myogenic differentiation[1-3]. Here we report that intragenic deletion of the dystrophin-encoding and muscular dystrophy-associated *DMD* gene is a frequent mechanism by which myogenic tumors progress to high-grade, lethal sarcomas. Dystrophin is expressed in nonneoplastic and benign counterparts for GIST, RMS and LMS, and the *DMD* deletions inactivate larger dystrophin isoforms, including 427kDa dystrophin, while preserving expression of an essential 71kDa isoform. Dystrophin inhibits myogenic sarcoma migration, invasion, anchorage independence, and invadopodia formation, and dystrophin inactivation was found in 96%, 100%, and 64% of metastatic GIST, RMS and LMS, respectively. These findings validate dystrophin as a tumor suppressor and likely anti-metastatic factor, suggesting that therapies in development for muscular dystrophies may also have relevance in treatment of cancer.

INTRODUCTION

1. Myogenic cancers are a **diverse** group of neoplasms, including rhabdomyosarcoma (RMS), leiomyosarcoma (LMS), and gastrointestinal stromal tumor (GIST).
2. Although presumptive initiating mutations have been identified in these cancers, the subsequent mechanisms of malignant progression and metastasis are not known.

GIST
- Gain-of-function mutations of *KIT* or *PDGFRA* are **initiating or at least early oncogenic events** in most GISTs, and such mutations are found even in premaligant microscopic GISTs.
- **Secondary mutations** associated with biologic progression from low-risk to high-risk GIST: *CDKN2A* inactivation or *TP53* inactivation.
- **Tertiary mutations** associated with progression from high-risk to metastatic GIST have not been identified.

RMS and LMS
- ~50% of embryonal RMS have RAS pathway mutations.
- ~50% of LMS have *TP53* or *PTEN* mutations.
- **Genetic determinants** for RMS and LMS progression and metastasis have not been identified.

MATERIALS & METHODS

DNA samples
High molecular weight genomic DNAs were isolated from a panel of 109 myogenic cancer patients.

SNP assay
The DNAs were analyzed using an Affymetrix 250K SNP array. DNA was digested with Nsp1, and linkers were ligated to the restriction fragments to permit PCR amplification. The PCR products were then purified and fragmented by treatment with DNase I. The fragmented PCR products were labeled and hybridized to microarray chips. The positions and intensities of the fluorescent emissions were analyzed using dChip software. Array intensity was normalized to the array with median intensity. Median smoothing was used to infer copy number.

Western blot
Frozen tumor samples were diced into small pieces in cold lysis buffer on dry ice and homogenized with a Tissue Tearor and the cell lysate was then rocked overnight at 4ºC. Lysate protein concentrations were determined using a Bio-Rad protein assay. The hybridization signals were detected by chemiluminescence and captured using a FUJI LAS1000-plus chemiluminescence imaging system.

Fluorescence in situ hybridization and Xist evaluation
BACs RP11-42E12 (*DMD*, chromosome Xp21.1) and RP11-939O17 (*DMD*, chromosome Xp21.1) were obtained from BAC/PAC Resources (Children's Hospital, Oakland, CA). A fosmid clone overlapping the *Xist* locus (G248P8779H11; Xq13.2) was obtained from BAC/PAC Resources (Children's Hospital, Oakland, CA). The fosmid DNA was labelled by nick translation with Spectrum Green-11-dUTP, and used in a triple-hybridization with the probes for *DMD* (spectrum orange) and centromere X (aqua).

MLPA
The MLPA procedure and capillary electrophoresis were conducted using the SALSA MLPA KIT P034-A2 / P035-A2 DMD / Becker from MRC-Holland.

Immunohistochemistry
IHC was performed on GIST/RMS/LMS sections following a standard protocol using Dys1 mouse monoclonal antibody (Novocastra).

Soft agar assay
Cells were plated in 35mm dishes after stable transfection of *EGFP* or *miniDMD* . The cells were incubated for 2-4 weeks and then stained with 1 ml of 0.005% Crystal Violet for 1 hour. Colonies were counted manually. All experiments were performed in triplicate.

Cell migration and invasion assay
Quantitative cell migration assays were performed using Matrigel-coated invasion inserts (BD Biosciences) and 8 mm pore membranes were used for invasion assays. Cells on the inside of the transwell inserts were removed with a cotton swab, and cells on the underside of the inserts were fixed and stained according to the protocol.

CONCLUSIONS

DMD is a tumor suppressor whose genomic inactivation is associated with progression to metastatic state in a diverse group of myogenic cancers.

RESULTS

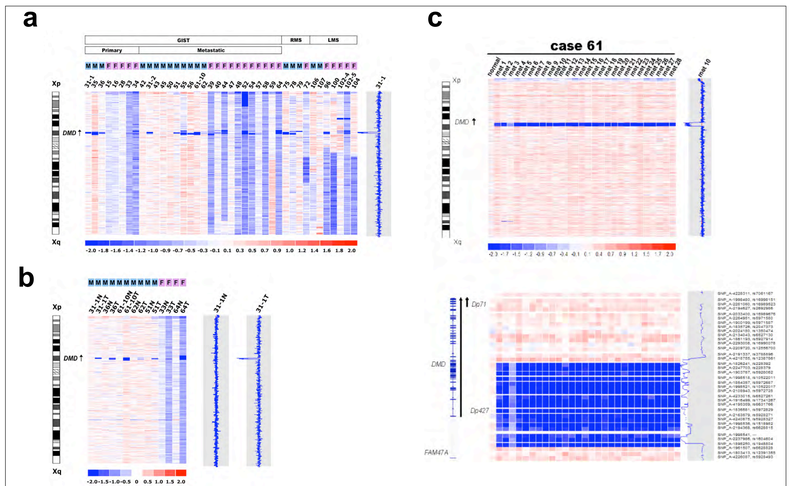

Fig. 1. Identification of somatic intragenic *DMD* deletions in human myogenic cancer
(a) dChip SNP log2 ratio copy number evaluations demonstrate intragenic *DMD* deletions in 25 of 40 (63%) primary or metastatic myogenic cancers. M denotes male and F denotes female .
(b) SNP evaluations in matched cancer and non-neoplastic cell DNAs from the same patients, demonstrating tumor-restricted nature of *DMD* deletions.
(c) Identical *DMD* deletions in each of 28 GIST metastases from patient 61. Top panel shows entire chromosome X; bottom panel focuses on the *DMD* locus. Data are shown as dChip SNP log2 ratio copy number, with a representative SNP profile (metastasis #10) shown at right.

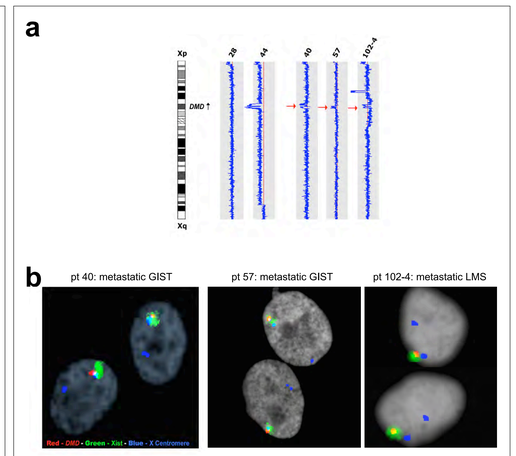

Fig. 2. *DMD* deletions in cancers from women.
(a) dChip SNP analyses in myogenic cancers from female patients, showing normal *DMD* copy number (case 28), nullizygous *DMD* deletion (case 44) and heterozygous *DMD* deletions (cases 40, 57, and 102-4).
(b) FISH and Xist analysis of metastatic GIST from 3 female patients showing *DMD* deletion in the Xist-negative active X chromosome. Probes are for *DMD* (red), X centromere (blue), and Xist (green).

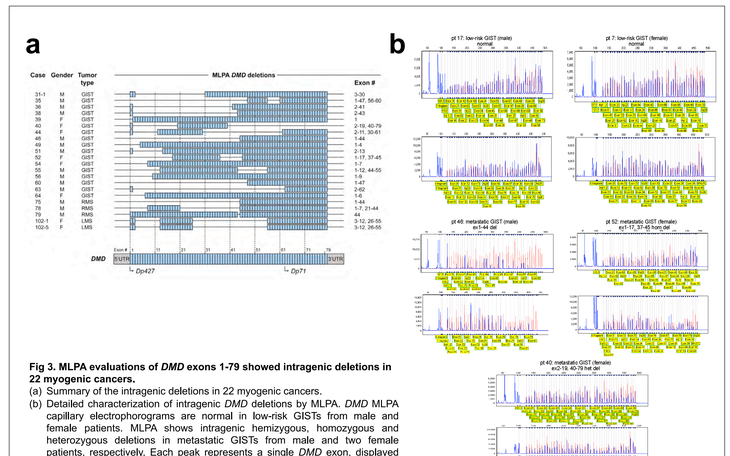

Fig 3. MLPA evaluations of *DMD* exons 1-79 showed intragenic deletions in 22 myogenic cancers.
(a) Summary of the intragenic deletions in 22 myogenic cancers.
(b) Detailed characterization of intragenic *DMD* deletions by MLPA. *DMD* MLPA capillary electrophorograms are normal in low-risk GISTs from male and female patients. MLPA shows intragenic hemizygous, homozygous and heterozygous deletions in metastatic GISTs from male and two female patients, respectively. Each peak represents a single *DMD* exon, displayed non-consecutively based on the size of the ligated stuffer sequence. The reference trace is shown in red, the tumor sample in blue.

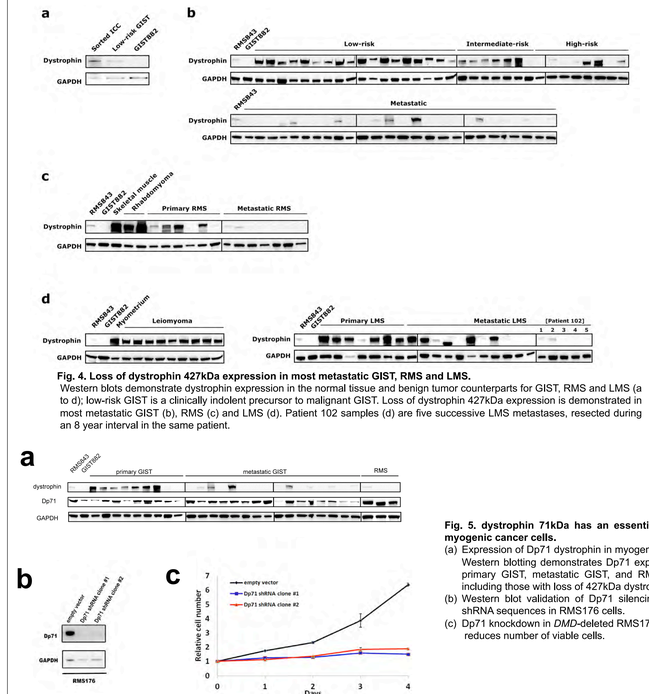

Fig. 4. Loss of dystrophin 427kDa expression in most metastatic GIST, RMS and LMS.
Western blots demonstrate dystrophin expression in the normal tissue and benign tumor counterparts for GIST, RMS and LMS (a to d); low-risk GIST is a clinically indolent precursor to malignant GIST. Loss of dystrophin 427kDa expression is demonstrated in most metastatic GIST (b), RMS (c) and LMS (d). Patient 102 samples (d) are five successive LMS metastases, resected during an 8 year interval in the same patient.

Fig. 5. dystrophin 71kDa has an essential role in myogenic cancer cells.
(a) Expression of Dp71 dystrophin in myogenic tumors. Western blotting demonstrates Dp71 expression in primary GIST, metastatic GIST, and RMS cases, including those with loss of 427kDa dystrophin.
(b) Western blot validation of Dp71 silencing by two shRNA sequences in RMS176 cells.
(c) Dp71 knockdown in *DMD*-deleted RMS176 reduces number of viable cells.

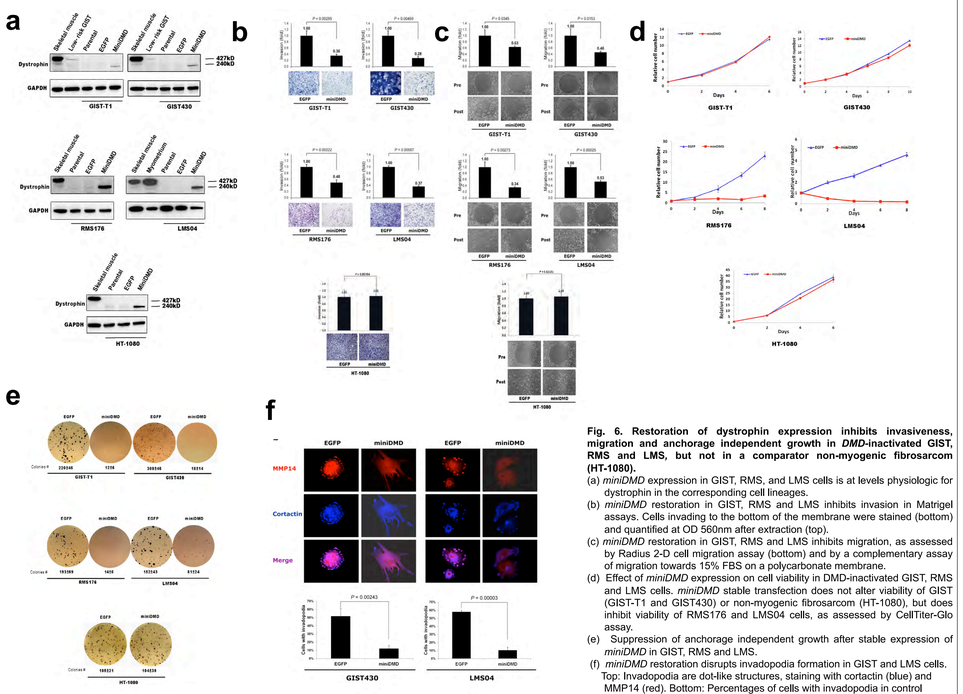

Fig. 6. Restoration of dystrophin expression inhibits invasiveness, migration and anchorage independent growth in *DMD*-inactivated GIST, RMS and LMS, but not in a comparator non-myogenic fibrosarcom (HT-1080).
(a) *miniDMD* expression in GIST, RMS, and LMS cells is at levels physiologic for dystrophin in the corresponding cell lineages.
(b) *miniDMD* restoration in GIST, RMS and LMS inhibits invasion in Matrigel assays. Cells invading to the bottom of the membrane were stained (bottom) and quantified at OD 560nm after extraction (top).
(c) *miniDMD* restoration in GIST, RMS and LMS inhibits migration, as assessed by Radius 2-D cell migration assay (bottom) and by a complementary assay of migration towards 15% FBS on a polycarbonate membrane.
(d) Effect of *miniDMD* expression on cell viability in DMD-inactivated GIST, RMS and LMS cells. *miniDMD* stable transfection does not alter viability of GIST (GIST-T1 and GIST430) or non-myogenic fibrosarcom (HT-1080), but does inhibit viability of RMS176 and LMS04 cells, as assessed by CellTiter-Glo assay.
(e) Suppression of anchorage independent growth after stable expression of *miniDMD* in GIST, RMS and LMS.
(f) *miniDMD* restoration disrupts invadopodia formation in GIST and LMS cells. Top: Invadopodia are dot-like structures, staining with cortactin (blue) and MMP14 (red). Bottom: Percentages of cells with invadopodia in control (EGFP vector) vs. dystrophin-restoration conditions.

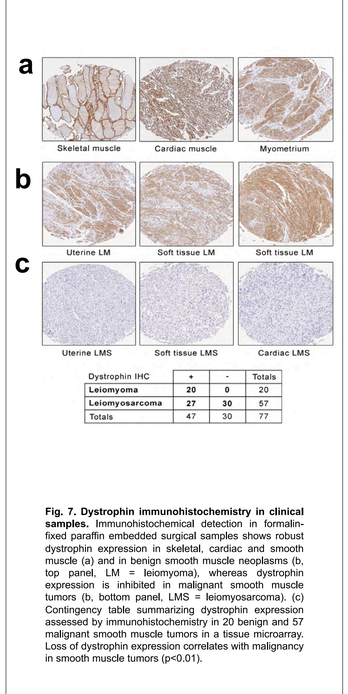

Dystrophin IHC	+	-	Totals
Leiomyoma	20	0	20
Leiomyosarcoma	27	30	57
Totals	47	30	77

Fig. 7. Dystrophin immunohistochemistry in clinical samples. Immunohistochemical detection in formalin-fixed paraffin embedded surgical samples shows robust dystrophin expression in skeletal, cardiac and smooth muscle (a) and in benign smooth muscle neoplasms (b, top panel, LM = leiomyoma), whereas dystrophin expression is inhibited in malignant smooth muscle tumors (b, bottom panel, LMS = leiomyosarcoma). (c) Contingency table summarizing dystrophin expression assessed by immunohistochemistry in 20 benign and 57 malignant smooth muscle tumors in a tissue microarray. Loss of dystrophin expression correlates with malignancy in smooth muscle tumors (p<0.01).